Bulletin of Volcanology (2019) 81: 32
https://doi.org/10.1007/s00445-019-1290-0

RESEARCH ARTICLE

The volcanic history of Pyrgousa—volcanism before the eruption of the Kos Plateau Tuff

David J. W. Piper[1] · Georgia Pe-Piper[2] · George Anastasakis[3] · Will Reith[2]

Received: 20 June 2018 / Accepted: 28 March 2019 / Published online: 24 April 2019

Abstract

The islet of Pyrgousa, 8 km west of Nisyros, has andesites overlain by proximal deposits of the Kos Plateau Tuff (KPT). These andesites record the evolution of the Kos-Nisyros volcanic centre prior to the large KPT eruption at 161 ka. This precursory activity had previously been recorded only in dacites and rhyolites in the Kefalos Peninsula, farther from the volcanic centre. This study investigated the age, geochemistry, mineralogy, and petrogenesis of the andesite domes, probable flows, and associated talus breccias on Pyrgousa. Analysed samples are basaltic andesite and andesite, with strong enrichment in Ba and Sr and low values of Ti and Zr. An $^{40}Ar/^{39}Ar$ date of 1.9 ± 0.1 Ma on biotite is similar to dates from dacite and rhyolite stocks and domes in the Kefalos Peninsula, and like those dates is the maximum age due to excess ^{40}Ar. There is no evidence on Pyrgousa for a stratovolcano precursor of the KPT eruption. The andesite domes geochemically resemble Pliocene domes in Methana and Aegina that mark the onset of magmatism in the northwestern South Aegean Arc, with an important magma component derived from subcontinental lithospheric mantle. These early andesites heated the upper crust, thus facilitating the growth of upper crustal magma chambers, which were filled by felsic crystal mush derived by differentiation of hydrous intermediate magmas with a more asthenospheric signature.

Keywords Andesite · Dome · South Aegean Arc · Nisyros · Subcontinental lithospheric mantle · Kos Plateau Tuff eruption

Introduction

Large rhyolite eruptions, such as the 161 ka Kos Plateau Tuff (KPT) eruption (Allen 2001; Bachmann et al. 2012), follow the accumulation of felsic crystal mush over 10^3–10^5 years in upper crustal (6–10 km deep) magma chambers. The rise of intermediate magma through the deeper crust above a subduction zone drives the volcanological system. The Kos-Nisyros volcanic centre provides an opportunity to examine the nature and role of early andesites as precursors to major felsic eruptions. Pre-eruption andesites play a role in heating and weakening the upper crust (Lipman 2007; Bachmann and Huber 2016), allowing the development of upper crustal magma chambers. The temporal variability of post-eruption intermediate magmas is well known (Bachmann et al. 2012; Barker et al. 2015; Klaver et al. 2017), but the evolution of pre-eruption andesites is less clear. In the case of the KPT eruption, the only records to date of pre-eruption andesites have been from enclaves preserved in dacite domes (Pe-Piper and Moulton 2008). In this study, we demonstrate the existence of pre-KPT andesites, show their mineralogical similarity to inclusions in early dacites, and contrast their bulk chemistry with post-eruption andesites. We argue that early andesites of the Kos-Nisyros system are similar to the oldest andesites in other centres of the South Aegean Arc in having a large component of magma derived from subcontinental lithospheric mantle.

Editorial responsibility: K.V. Cashman

Electronic supplementary material The online version of this article (https://doi.org/10.1007/s00445-019-1290-0) contains supplementary material, which is available to authorized users.

✉ David J. W. Piper
david.piper@canada.ca

[1] Natural Resources Canada, Geological Survey of Canada Atlantic, Bedford Institute of Oceanography, Dartmouth, NS B2Y 4A2, Canada

[2] Department of Geology, Saint Mary's University, Halifax, NS B3H 3C3, Canada

[3] Section of Historical Geology–Palaeontology, Department of Geology & Geoenvironment, National and Kapodistrian University of Athens, Panepistimiopolis, 15784 Zografou, Greece

The KPT eruption was the largest late Quaternary eruption in the eastern Mediterranean (Allen 2001; Bachmann et al. 2012). The only records of volcanism prior to the KPT are dacites and rhyolites on the Kefalos Peninsula of western Kos (Pe-Piper and Moulton 2008; Bachmann et al. 2010b), and more mafic rocks on Pyrgousa and the nearby islet of Pachia (Fig. 1). Nisyros Volcano was constructed after the KPT eruption (Hunzicker and Marini 2005). Based on comparison of the Kefalos Peninsula felsic rocks with post-KPT rocks on Nisyros, Bachmann et al. (2012) argued that dacitic eruptive products changed from hornblende-biotite magmas with lower eruption temperatures before the KPT to drier, more pyroxene-rich magmas with higher eruption temperatures after the KPT, as a result of loss of volatiles during the

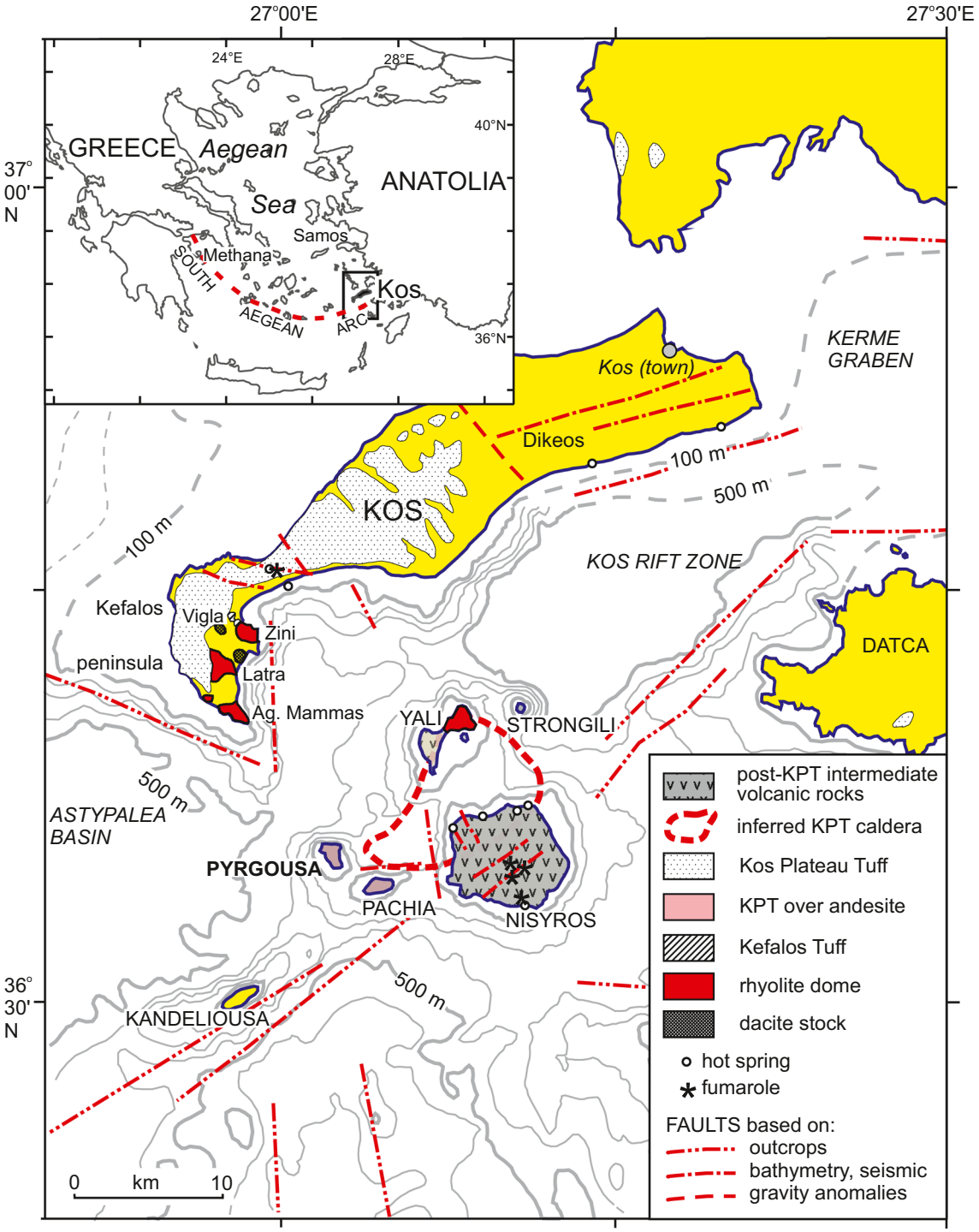

Fig. 1 Regional geological map of the Nisyros volcanic centre showing the location of Pyrgousa. Inset shows location in the Aegean Sea and South Aegean Arc

KPT eruption. This eruption partly emptied a magma chamber at 6–10 km depth (Bachmann et al. 2010b). All erupted rocks had an intermediate (andesitic) parent magma that evolved principally by crystal fractionation, following a wet, high oxygen fugacity liquid line of descent that is common in subduction zones (Bachmann et al. 2012).

The uninhabited islet of Pyrgousa (Fig. 2), 1.5 × 1 km, is located 8 km west of the late Quaternary volcanic centre of Nisyros Island. In the literature, Pyrgousa (Greek Πυργουσα) has been reported as Pergousa, Pergoussa, Perigusa, Pyrgussa, and Pyrgoussa. We use Pyrgousa for consistency with the Global Volcanism Program. On Pyrgousa, andesites of unknown age and affinity (Di Paola 1974) are overlain by proximal deposits of the KPT. These andesites provide an opportunity to understand the petrogenetic development of less differentiated magmas prior to the major caldera collapse in the KPT eruption (Allen 2001; Bachmann et al. 2012). They constrain the nature of the build-up to the KPT eruption, including whether the KPT caldera destroyed an older stratovolcano. This study investigated the age, geochemistry, and petrogenesis of this pre-KPT volcanism and made incidental observations on the KPT deposits and the overlying marine isotope stage (MIS) 5e carbonate-rich raised terrace.

Geological setting

Pliocene and earlier Pleistocene volcanism of the Nisyros-Kos region is represented by shallow dacite stocks and rhyolite domes on the Kefalos Peninsula of southwestern Kos (Fig. 1). Reported ages range from 2.6 to 0.5 Ma (Bellon and Jarrige 1979; Pasteels et al. 1986; Matsuda et al. 1999), but Bachmann et al. (2010a) showed that these dates are too old

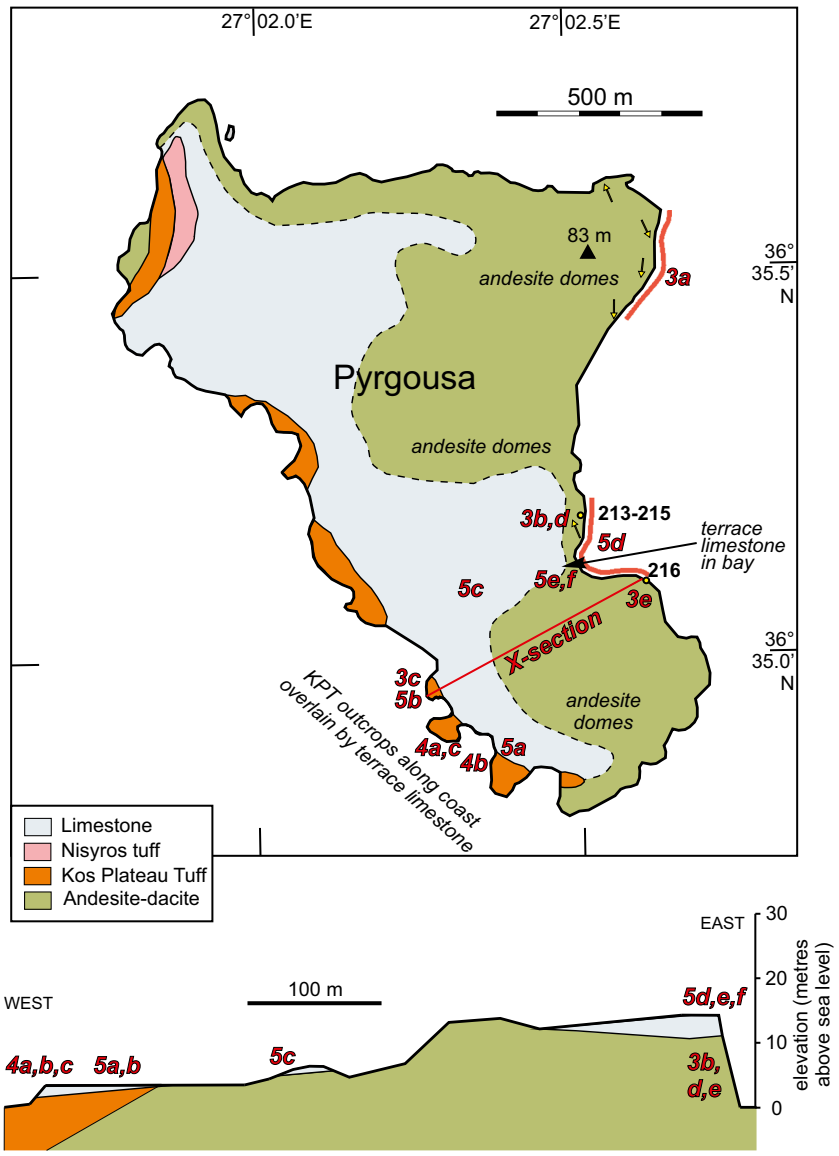

Fig. 2 Map and schematic cross section of Pyrgousa showing location of samples and Figs. 3, 4, 5. Based on IGME (2003), with modifications from Nomikou et al. (2018) and our field observations

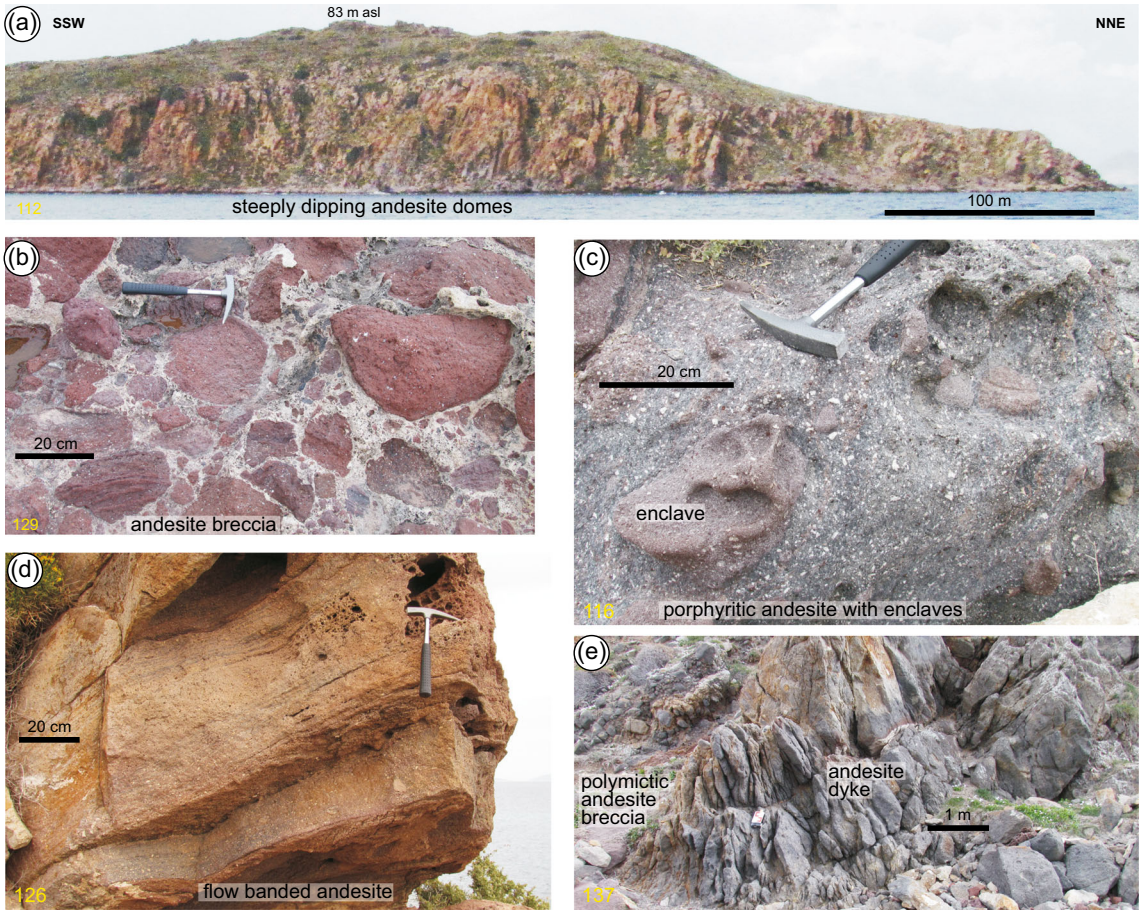

Fig. 3 Photographs of igneous basement lithologies. **a** Northeast coast of islet showing steeply dipping andesite domes. **b** Andesite breccia. **c** Porphyritic andesite. **d** Flow banded andesite dipping 30°N. **e** Dyke cutting polymictic andesite breccia. Hammer is 27 cm long, notebook 18 cm long

due to excess ^{40}Ar. Dating of non-inherited zircons from the Agios Mammas and Zini rhyolite domes gave ages of ~ 0.3 and ~ 0.5 Ma, respectively (Bachmann et al. 2010a), in contrast to Pliocene K-Ar and Ar-Ar ages for Agios Mammas (Bellon and Jarrige 1979; Bachmann et al. 2010a). These rocks are hornblende and biotite rich with low eruption temperatures (~ 750–800 °C; Bachmann et al. 2012). They were followed by build up of magma over a period of 200 ka (Bachmann et al. 2007) culminating in the 0.16 Ma KPT eruption (Allen 2001), centred on the marine area between Yali and Nisyros. This eruption ejected ~ 60 km^3 of rhyolite magma and ~ 3 km^3 of lithic debris (DRE) from the vent and conduit (Allen 2001), including older andesitic lavas transported as lithic clasts (Pe-Piper and Moulton 2008).

The volcanic islands of Nisyros, Yali, and Strongili (andesite-rhyolite; Fig. 1) have been constructed entirely since the eruption of the KPT and bound the likely source caldera of the KPT (Hunzicker and Marini 2005). To the southwest, the caldera is bounded by tiny remnants of the pre-eruption andesites in the islets of Pachia and Pyrgousa. Modern geochemical and isotopic analyses are available only from Nisyros and Yali (Wyers and Barton 1989; Francalanci et al. 1995; Buettner et al. 2005; Vanderkluysen et al. 2005). Both the Kefalos and Nisyros silicic rocks evolved from magmas of intermediate composition, with high Sr/Y (~ 40) and Nb < 20 ppm (Bachmann et al. 2012).

The first modern work on Pyrgousa was by Di Paola (1974) who reported "porphyritic andesite lava flows, covered with Quaternary reef limestones and in the south, pumiceous tuff." The IGME (2003) 1:25,000 map and modifications by Nomikou et al. (2018) show the distribution of the KPT all along the west coast of the islet (Fig. 2). Blackwell et al. (2016) make passing mention of a Late Pleistocene calc-alkaline lava, the Kyra tephra from Nisyros, and the Yali Upper Pumice all being present in northern Pyrgousa. None of these units was found in our work on the southern part of the islet.

The lithostratigraphy of the KPT on Pyrgousa has not been previously reported. Allen (1998) described only lithic clasts apparently derived from the KPT in beachrock. The KPT is better known on the nearby islet of Pachia, where Allen (1998) identified units A, C, and D of the KPT overlying 10 cm of unconsolidated mud, interpreted as showing deposition of the KPT over a swamp or dry land.

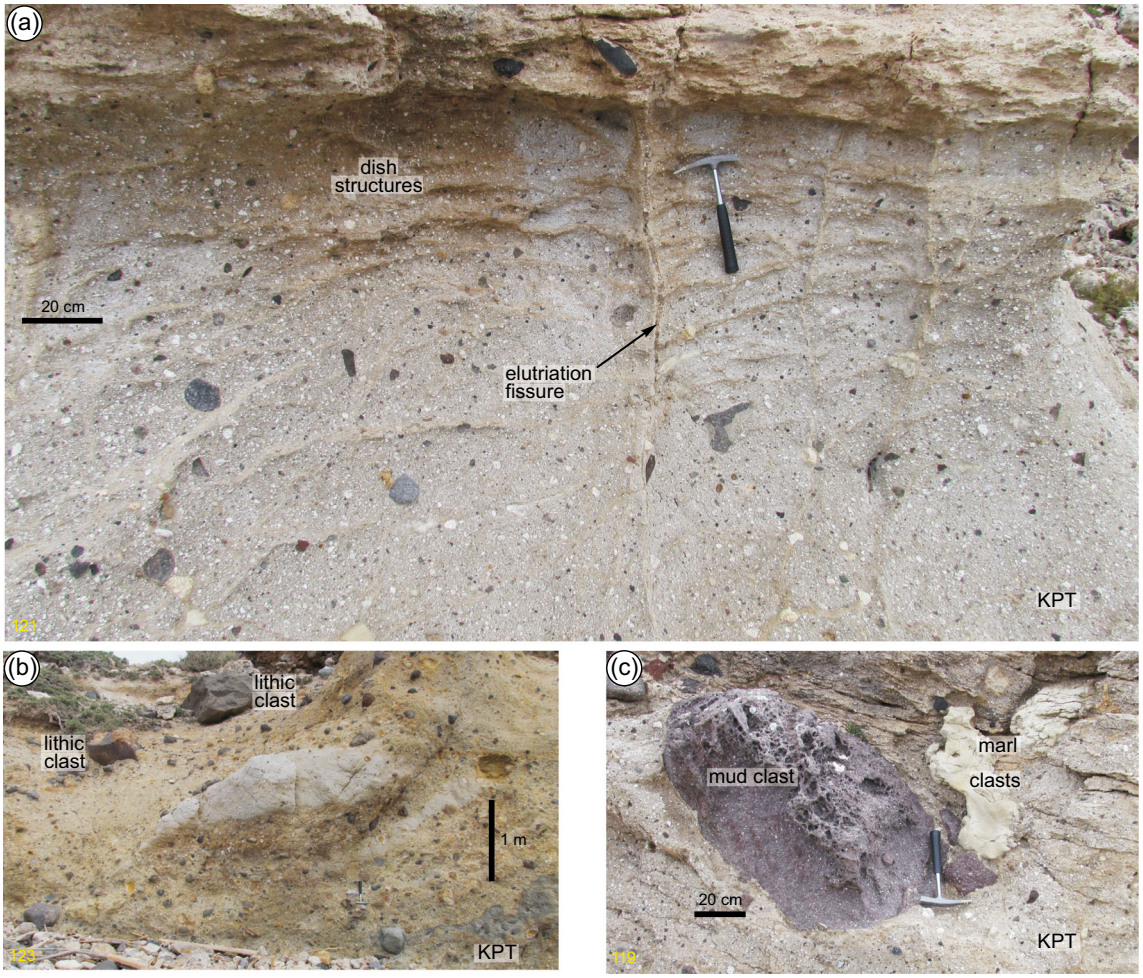

Fig. 4 Photographs of Kos Plateau Tuff. **a** Top of KPT on southwest coast, showing character of lithic (dark) and vitric (white) clasts and elutriation textures. **b** Large lithic clasts at top of KPT on southwest coast. **c** Large clasts of dark mud and light grey marl, top of KPT, southwest coast

Methods

We examined the cliffs on the northeast of Pyrgousa from photographs taken from our boat and we also made an E–W transect of the southern part of the islet (Fig. 2), examining in detail the fresh outcrops at the shoreline. Igneous rock samples were analysed for both major and trace elements by Activation Laboratories Ltd. (Ancaster, Canada) according to their codes 4Lithoresearch and 4B1, which combine lithium metaborate/tetraborate fusion ICP analyses with a trace element ICP-MS package. Rock textures and minerals were studied by scanning electron microscope (SEM) and mineral chemistry was determined by energy dispersive spectroscopy (EDS). Analyses with poor totals or > 2% contamination by non-stoichiometric elements were excluded: criteria are summarised in Table 2 of Pe-Piper et al. (2016). The EDS system uses a single cobalt standard, and precision is better than 1% for elements above Ne in the periodic table. EDS analyses are from a larger spot (~ 10 μm) than WDS and gives poor accuracy for elements present at < 1%. For major elements, accuracy compared to WDS analyses is better than 5%.

One composite biotite separate was dated by the $^{40}Ar/^{39}Ar$ technique by Geochronex Analytical Services Ltd. (Burlington, Canada). The biotite sample was wrapped in Al foil and loaded in an alumina vial with LP-6 flux monitors. A batch of samples and monitors were irradiated and flux monitors were run. The Ar isotope composition was measured in a Noblesse Noble Gas static mass spectrometer (NU Instruments Ltd., Wrexham, UK). A 1300 °C blank of ^{40}Ar did not exceed $n \times 10^{-11}$ cc at standard temperature and pressure.

Results

Field observations

Most of the eastern coastline of Pyrgousa exposes andesite domes, probable lesser flows, and associated talus breccias

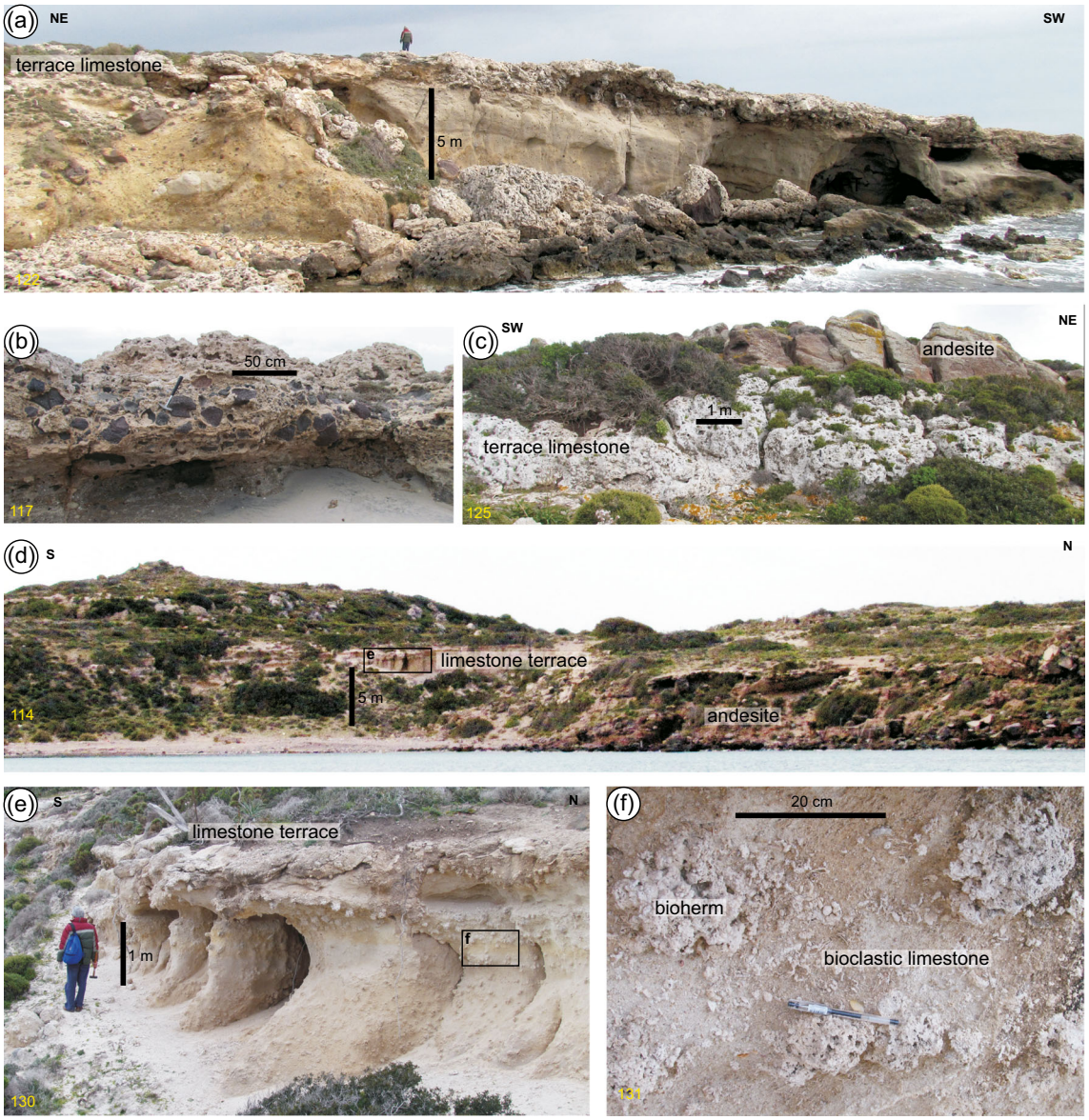

Fig. 5 Photographs of raised limestone terraces. **a** Terrace limestone over KPT on southwest coast. **b** Detail of beachrock with andesite cobbles, overlain by karstic limestone, southwest coast, unconformably overlying KPT. **c** Paleo-islet of andesite, surrounded by karstic limestone. South-central Pyrgousa. **d** Elevated limestone terrace in bay on southeast coast. **e** Cliff in bioclastic limestone at **d**. **f** Bioherms in bioclastic limestone at **e**

and minor dykes (Fig. 3). Marginal dips on domes, in places picked out by flow banding (Fig. 3d), are locally as steep as 70° (Fig. 3a). Some talus breccia is monomictic, some polymictic (Fig. 3e), and some has an apparently felsic pyroclastic matrix (Fig. 3b). The andesite is variably porphyritic and includes enclaves (Fig. 3c). There is no evidence for a stratified build-up of flows and pyroclastic deposits.

The KPT unit on Pyrgousa comprises massive, structureless tuff with dispersed pumice and lithic clasts generally < 5 cm in size (Fig. 4a). Near the top of the unit, lithic (volcanic) clasts are up to 1 m in size (Fig. 4b) and blocks both of mud and marl are > 0.5 m (Fig. 4c). Elutriation fissures are present near the top of the unit, together with structures that resemble dish structures (cf. Lowe 1975) in turbidites (Fig. 4a). The basal contact of the KPT was not found and the maximum exposed thickness is about 7 m (Fig. 5a).

Limestones unconformably overlie the andesites and KPT, forming a morphological terrace at 8–10 m above sea level in the southeast of the islet (Fig. 5d), and from 6 m to close to modern sea level in the southwest (Fig. 5a). The terrace locally includes bioclastic limestone (Fig. 5e) with small bioherms (Fig. 5f). In the southwest, cobble conglomerate with a limestone matrix (Fig. 5b), interpreted as beachrock, unconformably overlies KPT. The uppermost limestone is karstic (Fig. 5b) and onlaps the higher andesite domes (Fig. 5c).

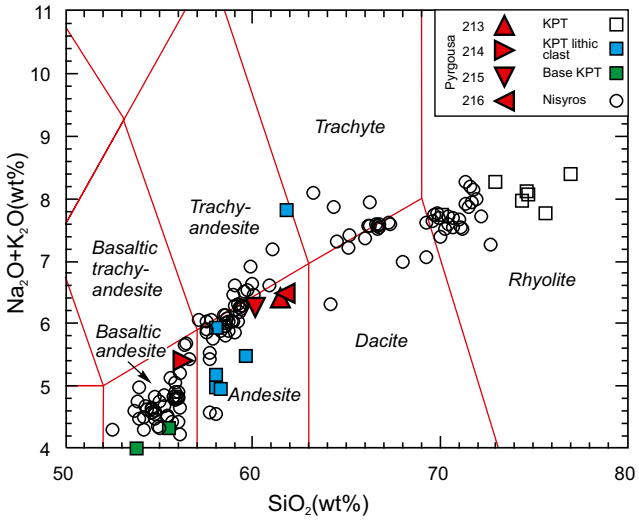

Fig. 6 TAS diagram showing Pyrgousa rocks and comparison with KPT bulk rock and lithic clasts (Pe-Piper and Moulton 2008), base of KPT (Piper et al. 2010), and post-KPT rocks of the Nisyros stratovolcano (Vanderkluysen et al. 2005)

Whole rock geochemistry

Four samples were analysed geochemically: three andesites and one basaltic andesite (sample 214) (Fig. 6; Table 1). Comparison is made with late Quaternary basaltic andesite and andesite from Nisyros (Vanderkluysen et al. 2005), basaltic andesite from pumice rafts immediately underlying the base of the KPT in southern Kos (Piper et al. 2010), and andesitic lithic clasts from unit E of the KPT (Pe-Piper and Moulton 2008).

Pyrgousa basaltic andesite has higher total alkalis (Fig. 6) than late Quaternary basaltic andesite from Nisyros and the base of the KPT and also differs in other elements (Fig. 7). Ni is lower than Nisyros and the base of the KPT, whereas K_2O is higher. Zr is between Nisyros and base-of-KPT values. Na_2O is similar to Nisyros, but higher than in basaltic andesite at the base of the KPT. The Pyrgousa andesites are noticeably rich in Ba (750–900 ppm) and Sr (700–800 ppm; Sr/Y = 33–40, Table 1) compared to Nisyros rocks, basaltic andesite from the base of the KPT, and some of the andesite clasts in the KPT. The Pyrgousa andesites resemble a dacite lithic clast in the KPT, which has Ba ~ 1100 ppm and Sr ~ 900 ppm (Pe-Piper and Moulton 2008), and the dacite stocks and rhyolite domes of the Kefalos Peninsula, which have Sr/Y ~ 40 (Bachmann et al. 2012).

Mineralogy and petrology

Petrologically, the basaltic andesite and andesite show generally similar features. The rocks are porphyritic, with phenocrysts and microphenocrysts of feldspar, amphibole, biotite, ± pyroxene. The groundmass is principally feldspar and glass, with some pyroxene, biotite, quartz, titanomagnetite, and amphibole. Mineral chemistry and classification are summarised in Figs. 8 and 9.

Basaltic andesite has subhedral to anhedral plagioclase phenocrysts, ranging in composition from bytownite to andesine (Fig. 9a, d; Fig. 10). Feldspar phenocrysts contain inclusions of F-apatite and magnesiohornblende (Fig. 10a). Other phenocrysts include magnesiohornblende, tschermakite and pargasite (Fig. 8a, b) altered to actinolite (Fig. 10c, f); ilmenite, titanomagnetite, zoned orthopyroxene (En_{74} to En_{63}; Fig. 8d; Fig. 10e) and rare quartz (Fig. 10d). The hornblende phenocrysts contain feldspar and F-apatite inclusions (Fig. 10f). In addition, only the basaltic andesite contains sanidine and anorthoclase (Figs. 9a, 10e) and local interstitial quartz (Fig. 10e). Microphenocrysts include anorthoclase (Fig. 10e), titanomagnetite, orthopyroxene (Fig. 10e), and pargasite (Fig. 10b). Euhedral biotite is very rare, but a large biotite with a reaction rim and inclusions of ilmenite appears to be a xenocryst (Fig. 10d). Glass is abundant in the groundmass and also occurs as inclusions in feldspar and amphibole phenocrysts.

Andesites have plagioclase phenocrysts principally of andesine, with some oligoclase and with labradorite cores (Fig. 9b, d; Fig. 11d, f, g). Spongy cellular rims and mantles (Fig. 11e) are better developed compared to the basaltic andesite. Pyroxenes are augite and enstatite-hypersthene (Fig. 8d). Clinopyroxene phenocrysts have dissolution voids and are rimmed by titanomagnetite, labradorite, and orthopyroxene (Fig. 11a), suggesting either magma mixing, or that the clinopyroxene is a xenocryst. Amphiboles are magnesiohornblende and edenite (Fig. 8a, b; Fig. 11c), probably implying lower pressure conditions than the basaltic andesite that contains pargasite (cf. Ridolfi et al. 2010). Biotite is more abundant than in basaltic andesite, being mostly of phlogopite composition, with higher ^{iv}Al than in the basaltic andesite (Fig. 8c). Biotite phenocrysts show reverse zoning and have voids and inclusions of titanomagnetite, F-apatite, and andesine (Fig. 11b).

There is widespread evidence of magma mixing from mineral textures in both basaltic andesite and andesite. Plagioclase phenocrysts show cores with quite different compositions from rims, separated by zone of spongy cellular texture with abundant voids (Fig. 11d–f). Some oligoclase-andesine crystals have narrow calcic spikes and patches of labradorite or bytownite (Fig. 11d, g), which may represent earlier clots of calcic plagioclase that have been substantially corroded and assimilated. Some plagioclase phenocrysts show oscillatory zoning from andesine to labradorite. Others show oligoclase cores followed by labradorite rims (Fig. 11f). Clinopyroxene phenocrysts appear to have reaction rims and may be xenocrysts (Fig. 11a). Similar magma mixing textures in dacites are described in more detail from the Kefalos Peninsula on Kos, 10 km to the NNW (Pe-Piper and Moulton 2008).

Table 1 Geochemical analysis of basaltic andesite and andesite, Pyrgousa

Oxide	Sample				Detection limit
	CS214 Basaltic andesite	CS215 Andesite	CS213 Andesite	CS216 Andesite	
Major elements, weight %, recalculated volatile free					
SiO_2	56.27	60.17	61.44	61.74	0.01
TiO_2	0.84	0.78	0.77	0.63	0.001
Al_2O_3	18.77	17.98	17.96	17.32	0.01
Fe_2O_{3T}	7.01	5.64	5.53	5.32	0.01
MnO	0.11	0.10	0.09	0.10	0.001
MgO	3.60	2.88	1.95	2.53	0.01
CaO	7.65	5.90	5.56	5.52	0.01
Na_2O	3.50	3.98	4.01	4.03	0.01
K_2O	1.92	2.29	2.41	2.45	0.01
P_2O_5	0.22	0.20	0.20	0.24	0.01
LOI	1.03	1.17	1.42	1.55	0.01
Total	100.1	100.7	98.34	99.68	0.01
Trace elements, ppm					
S	0.014	0.011	0.006	0.017	0.001
V	189	128	142	124	5
Co	18	15	13	12	1
Ni	12	7	7	10	1
Cu	53	30	37	20	1
Zn	53	46	44	59	1
Sc	20	16	15	11	1
Ga	18	18	18	18	1
Rb	48	57	59	61	1
Ba	763	758	781	878	3
Cs	1.4	2.3	1.1	2.9	0.1
Sr	809	729	693	754	2
Y	20.7	19.7	20.8	19	0.5
Zr	139	147	156	157	1
Nb	9.9	12.5	12.9	12.4	0.2
Hf	3.2	3.4	3.7	3.6	0.1
Ta	0.59	0.88	0.89	0.86	0.01
W	1.3	1.4	1.2	1.2	0.5
Tl	0.06	0.08	0.09	0.23	0.05
Pb	8	8	9	11	3
Th	4.45	8.7	8.97	9.13	0.05
U	1.51	2.54	2.74	2.81	0.01
La	27.3	34.6	36.2	37.9	0.05
Ce	52.6	64	62.7	70.4	0.05
Pr	5.67	6.62	6.81	7.37	0.01
Nd	21.3	24.2	24.5	26.4	0.05
Sm	3.97	4.31	4.24	4.41	0.01
Eu	1.15	1.17	1.2	1.19	0.005
Gd	3.53	3.63	3.6	3.41	0.01
Tb	0.56	0.55	0.56	0.51	0.01
Dy	3.34	3.15	3.17	3.06	0.01
Ho	0.68	0.65	0.65	0.61	0.01

Table 1 (continued)

Oxide	Sample				Detection limit
	CS214 Basaltic andesite	CS215 Andesite	CS213 Andesite	CS216 Andesite	
Er	2.07	1.96	1.93	1.84	0.01
Tm	0.303	0.295	0.294	0.279	0.005
Yb	2.04	1.91	1.93	1.83	0.01
Lu	0.304	0.293	0.299	0.287	0.002
Sr/Y	39.1	37.0	33.3	39.7	

The chemistry of the major minerals is compared with the Kefalos Peninsula dacites and rhyolites and lithic clasts from the KPT (Pe-Piper and Moulton 2008). Clinopyroxene is augite and is more ferroan than most clinopyroxene from lithic clasts in the KPT, where compositions are more calcic and include common diopside (Fig. 8d). Amphibole compositions are similar to those in the Vigla dacite and its andesite enclaves, except for the low-Si amphiboles, which are pargasite on Pyrgousa and the more ferroan magnesiohastingsite at Vigla.

Geochronology

$^{40}Ar/^{39}Ar$ dating of a biotite separate from sample CS216 yielded a total gas age of 2.1 ± 0.1 Ma (Supplementary Table 1), and an inverse isochron age of 1.7 ± 2.8 Ma with a good plateau at 1.9 ± 0.1 Ma (Fig. 12). The initial $^{40}Ar/^{36}Ar$ intercept is 307 ± 32, rather higher than the atmospheric ratio of 295.5.

Discussion

Age and volcanological character of the pre-KPT andesites

Our $^{40}Ar/^{39}Ar$ dating results are similar to those of Bachmann et al. (2010a) in having an elevated $^{40}Ar/^{36}Ar$ intercept with a large error and a somewhat disturbed age spectrum. It is therefore likely that the biotite has excess ^{40}Ar of mantle origin, as argued by Bachmann et al. (2010a). In this case, the 1.9 ± 0.1 Ma age should be taken as a maximum possible age.

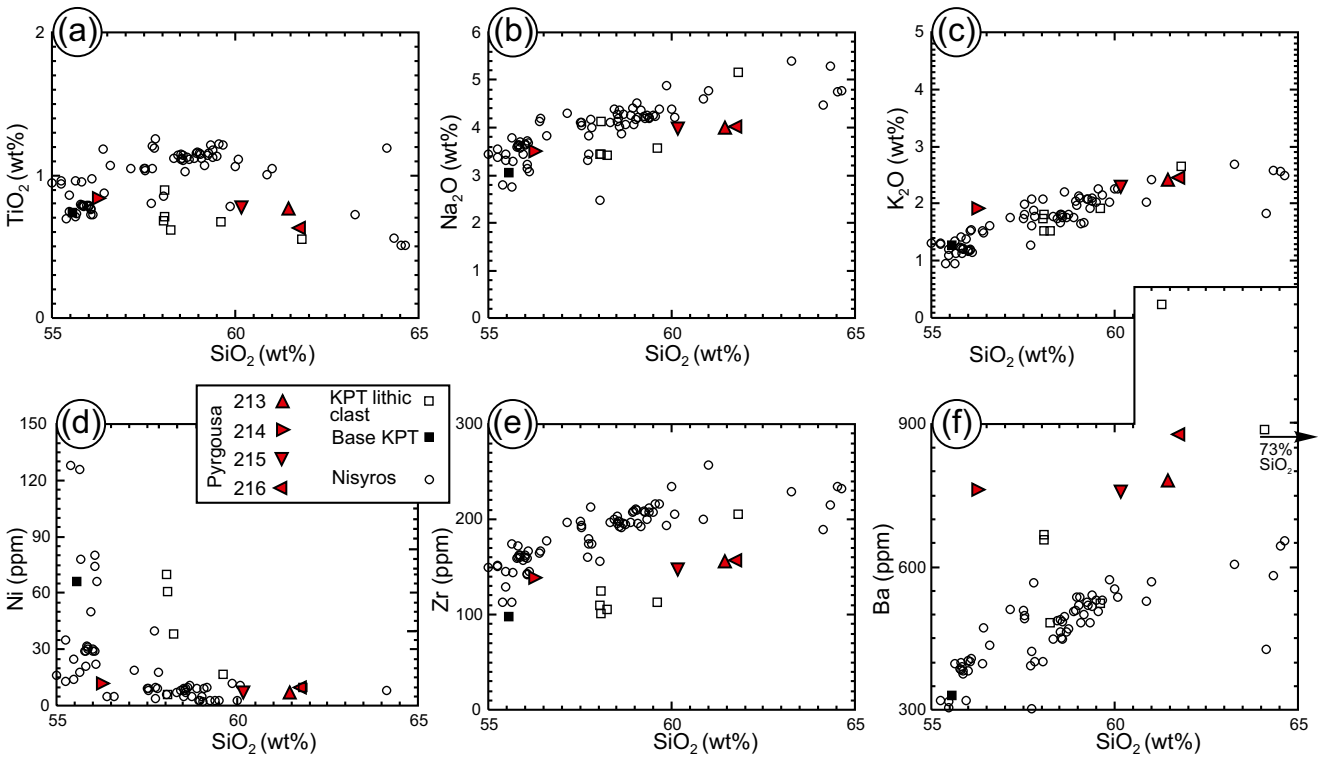

Fig. 7 Variations of selected elements with SiO_2 for Pyrgousa rocks and regional comparisons (sources as in Fig. 6)

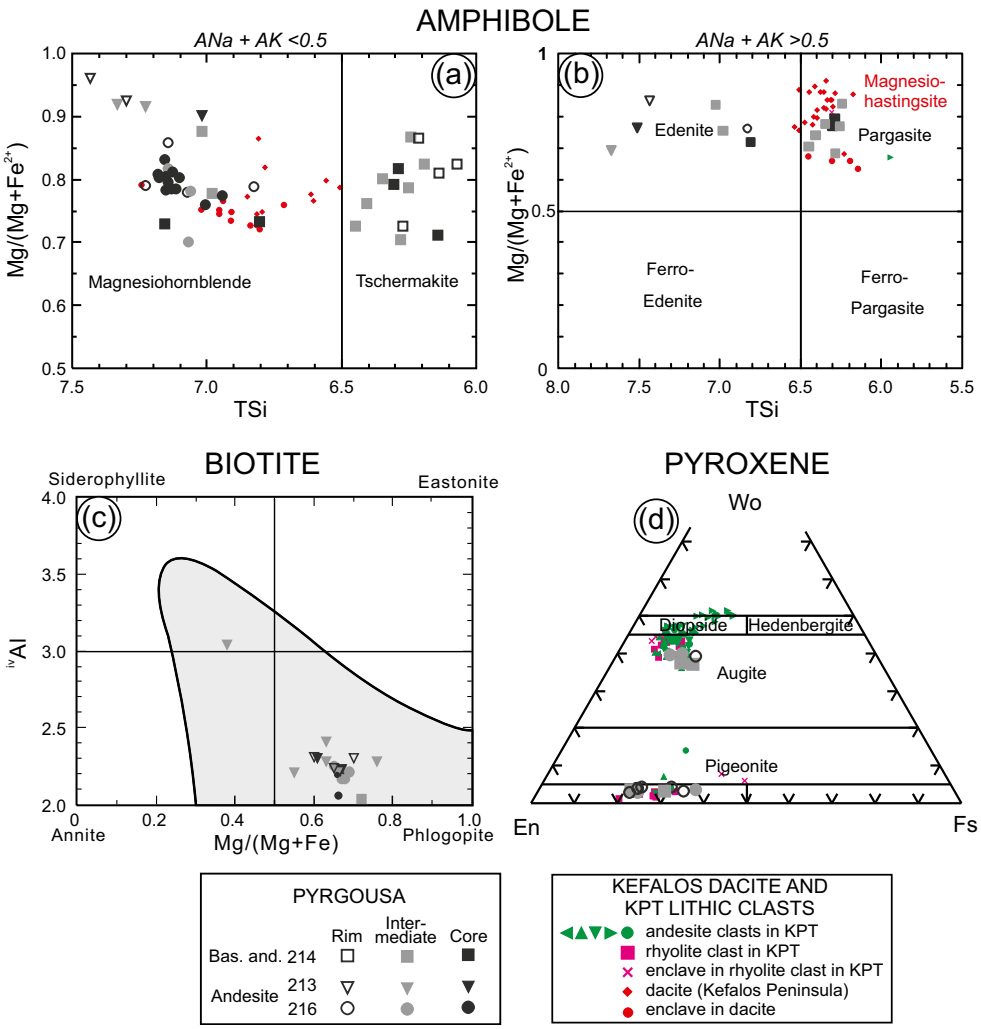

Fig. 8 Mineral chemistry of the Pyrgousa rocks. **a**, **b** Amphibole; **c** biotite; **d** pyroxene. Coloured symbols are mineral analyses of Pe-Piper and Moulton (2008) from the Vigla dacite and lithic clasts in the KPT

Nevertheless, our field observation that the andesites occur principally as domes (Fig. 3a) is important, as there is no evidence for a stratovolcano of interbedded lavas and pyroclastic rocks prior to the KPT eruption. The volcanological evolution of the Nisyros-Kos volcanic system in the Quaternary resembles the Pliocene–Quaternary history of the Methana volcanic system in the northwestern part of the South Aegean Arc (Pe-Piper and Piper 2013). There, small domes of andesite-dacite were widespread in the late Pliocene and were followed by a 1–3-Ma period of erosion prior to the development of a central explosive volcanic centre (unit C of Pe-Piper and Piper 2013) and then younger Quaternary stratovolcanoes. How much erosion may have taken place on Pyrgousa prior to the KPT eruption is unclear.

Petrogenesis of the Pyrgousa basaltic andesite and andesite

The widespread evidence of complex irregular zoning in phenocrysts is similar to that described from the Kefalos Peninsula by Pe-Piper and Moulton (2008), resulting from mixing within a magma chamber and changing conditions during rise of magma to the surface (Ridolfi et al. 2010). Similar textures are known from other small volume magmas produced from subcontinental lithospheric mantle (SCLM), such as in the Upper Miocene of Samos (Pe-Piper and Piper 2007). The most pronounced evidence for mixing is in the basaltic andesite (CS214), where the abundance of bytownite-labradorite indicates a more mafic or more hydrous parent magma (Lange et al. 2009). Both phenocrystic and interstitial quartz (Fig. 10d, e) are present, together with apparently xenocrystic biotite (Fig. 10d). Both minerals are more characteristic of the probably coeval dacites and rhyolites of the Kefalos Peninsula. If this basaltic andesite involved mixing of a dacitic component, then the host magma of the bytownite-bearing component must have been quite mafic. This is contrary to the suggestion of Bachmann et al. (2012) that parent magmas were all of intermediate composition.

The andesite of Pyrgousa is similar to the putative parent intermediate magma postulated by Bachmann et al. (2012) for the pre-KPT dacites and rhyolites of the Kefalos Peninsula.

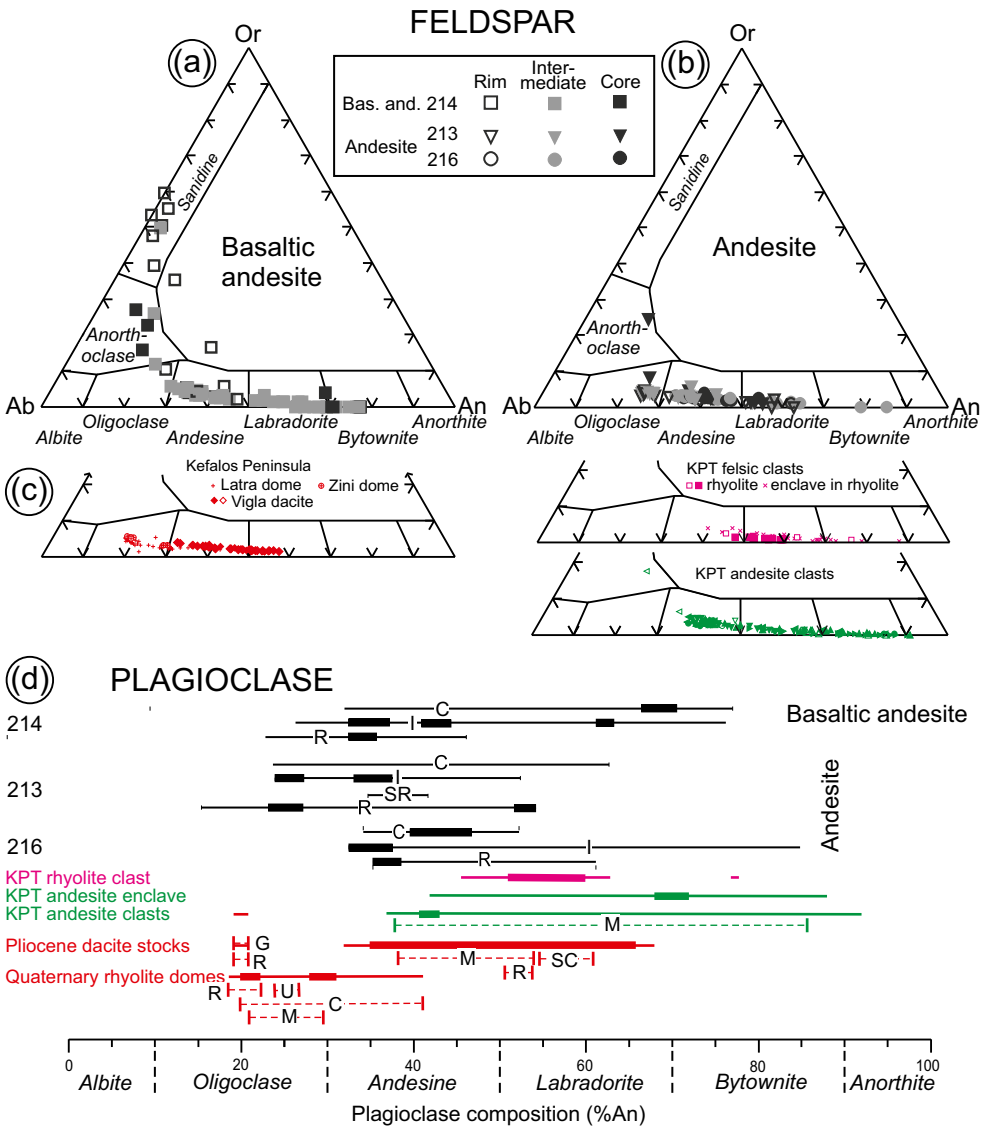

Fig. 9 Mineral chemistry of **a** feldspar in basaltic andesite; **b** feldspar in andesite; **c** feldspar from dacite stocks and rhyolite domes of the Kefalos Peninsula and lithic clasts in the KPT (Pe-Piper and Moulton 2008). **d** Compositional ranges in plagioclase for Pyrgousa rocks and comparative rocks from Pe-Piper and Moulton (2008). Thickness of line indicates relative abundance. C = core of phenocryst; I = intermediate zone of phenocryst; G = groundmass; M = microphenocryst; R = rim of phenocryst; SC = spongy cellular core of phenocryst; U = unzoned phenocryst

The andesites are geochemically distinct from younger basaltic andesite and andesite at the base of the KPT (Piper et al. 2010) and in the late Quaternary Nisyros stratovolcano (Vanderkluysen et al. 2005). They also differ in the chemistry of clinopyroxene (Fig. 8d). The Pyrgousa rocks are less enriched in HFSE such as Ti and Zr, but strongly enriched in Ba and Sr and to a lesser extent K, and show a high Sr/Y ratio of ~39. Similar trends are observed in the dacites and their andesitic enclaves at Vigla in the Kefalos Peninsula on Kos, 10 km to the NNW (Pe-Piper and Moulton 2008; Bachmann et al. 2012). The more ferroan low-Si amphiboles in the Vigla dacite compared to those from Pyrgousa (Fig. 8b) probably reflects changes in oxygen fugacity between andesitic and dacitic magmas.

The high Ba, Sr, and K contents of the Pyrgousa andesite and basaltic andesite resemble late Miocene plutonic and volcanic rocks from Samos, Bodrum, and Kos. These late Miocene rocks have been interpreted as derived from small degrees of partial melting from potassium-enriched SCLM. For example, in Samos, the SCLM was an enriched hydrous peridotite within the stability field of phlogopite, amphibole, and garnet with 5–10% partial melting and no significant dilution by asthenospheric melts (Pe-Piper and Piper 2007). Such high Sr-Ba rocks are widespread in the eastern Aegean, but absent in the west (Pe-Piper and Piper 2002). In the Kos-Nisyros region, the Nd and Sr isotopic signature is largely derived from subducted Nile River sediment (Pe-Piper and Moulton 2008; Klaver et al. 2015). The KPT and younger rocks of Nisyros lack enrichment in Sr and Ba and are isotopically characteristic of higher degrees of partial melting of depleted MORB mantle (DMM; Klaver et al. 2015). There is a similar pattern in the volcanic rocks of Methana (Fig. 1 inset), at the western end of the South Aegean Arc, where studies of Pb and Nd

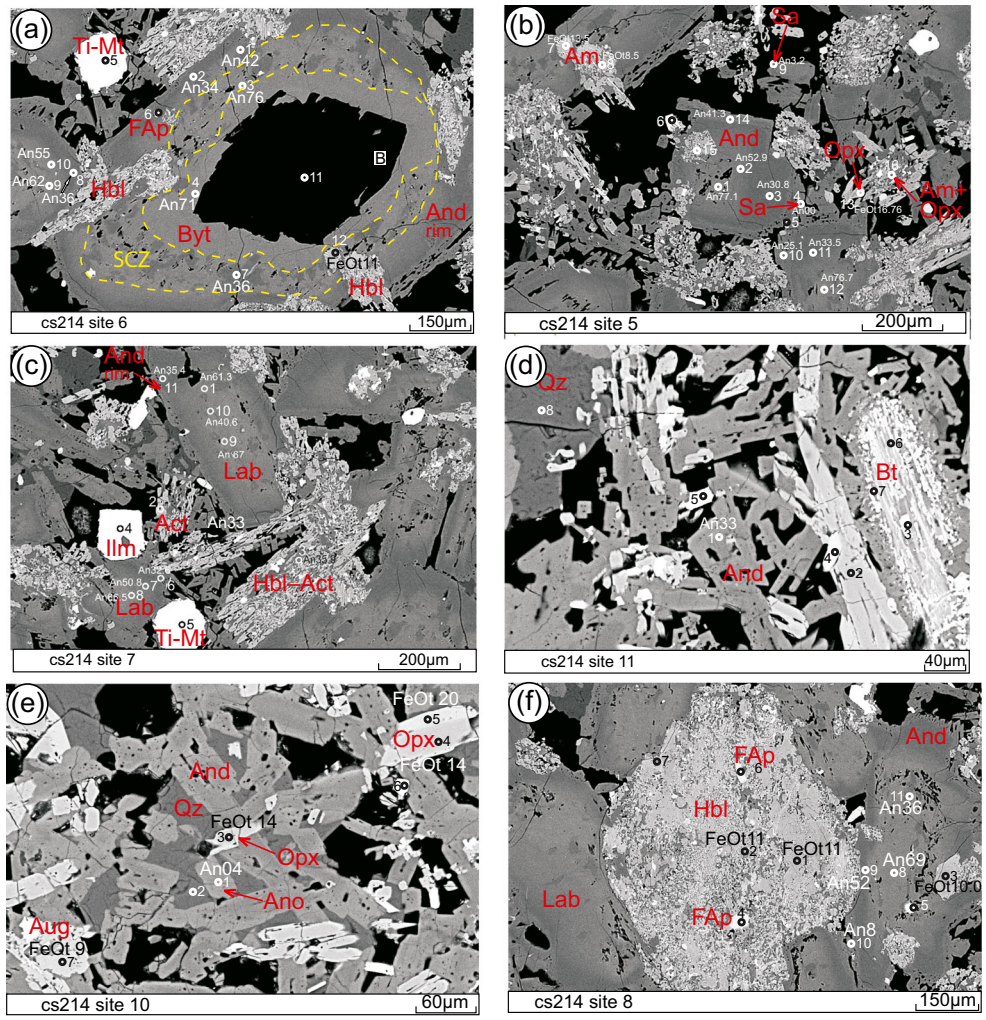

Fig. 10 Basaltic andesite mineral textures. Numbers refer to mineral analyses (See Supplementary Material). A content of feldspar and FeO content of ferromagnesian minerals are shown. Mineral abbreviations from Whitney and Evans (2010). **a** Hollow zoned plagioclase phenocrysts with bytownite-labradorite core, a spongy cellular zone (*SCZ*), and a wide andesine rim that has large inclusions of magnesiohornblende (12). **b** Zoned plagioclase phenocrysts from bytownite (1, 12) to andesine with sanidine rims (4, 9). Amphibole phenocrysts with orthopyroxene inclusions (15, 16) and orthopyroxene (13) and ilmenite (6) microphenocrysts. **c** Zoned plagioclase phenocrysts interlocked with hornblende partly altered to actinolite (2). Phenocrysts of ilmenite (4) and titanomagnetite (5). **d** Biotite (6, 7) xenocryst with ilmenite (3) exsolution. Phenocrysts of plagioclase (1) and quartz (8) both with voids. **e** Phenocrysts of zoned orthopyroxene (En_{74}–En_{63}) and plagioclase. Microphenocrysts of anorthoclase (1), titanomagnetite (6), and orthopyroxene (3). Interstitial quartz (2). **f** Large hornblende phenocryst with F-apatite inclusions (4, 6), pargasite microphenocrysts (3), titanomagnetite microphenocrysts (5), zoned plagioclase phenocrysts (labradorite (8) to andesine (9))

isotopes (Elburg et al. 2014; Smet 2014) show that the Pliocene domes have little or no DMM contribution and cannot be completely accounted for by Cenozoic sediment subduction (Klaver et al. 2015). By analogy with Kos-Nisyros, the early domes on Methana resulted from partial melting of SCLM prior to significant supply from asthenospheric mantle.

Character of the KPT deposit

The KPT deposit on Pyrgousa resembles unit Dm reported by Allen (1998) on Pachia islet, where the KPT overlies unconsolidated mud, apparently similar to the lithic clasts of mud on Pyrgousa (Fig. 4c). This underlying mud is consistent with the interpreted absence of a stratovolcano prior to the KPT eruption. Distally on Kos, the KPT is commonly underlain by vegetated paleosols (Allen et al. 1999).

Origin and significance of the terrace limestones

Terrace limestone with marine fossils unconformably overlies the KPT and represents a marine highstand after the likely subaerial eruption of the KPT (cf. observations

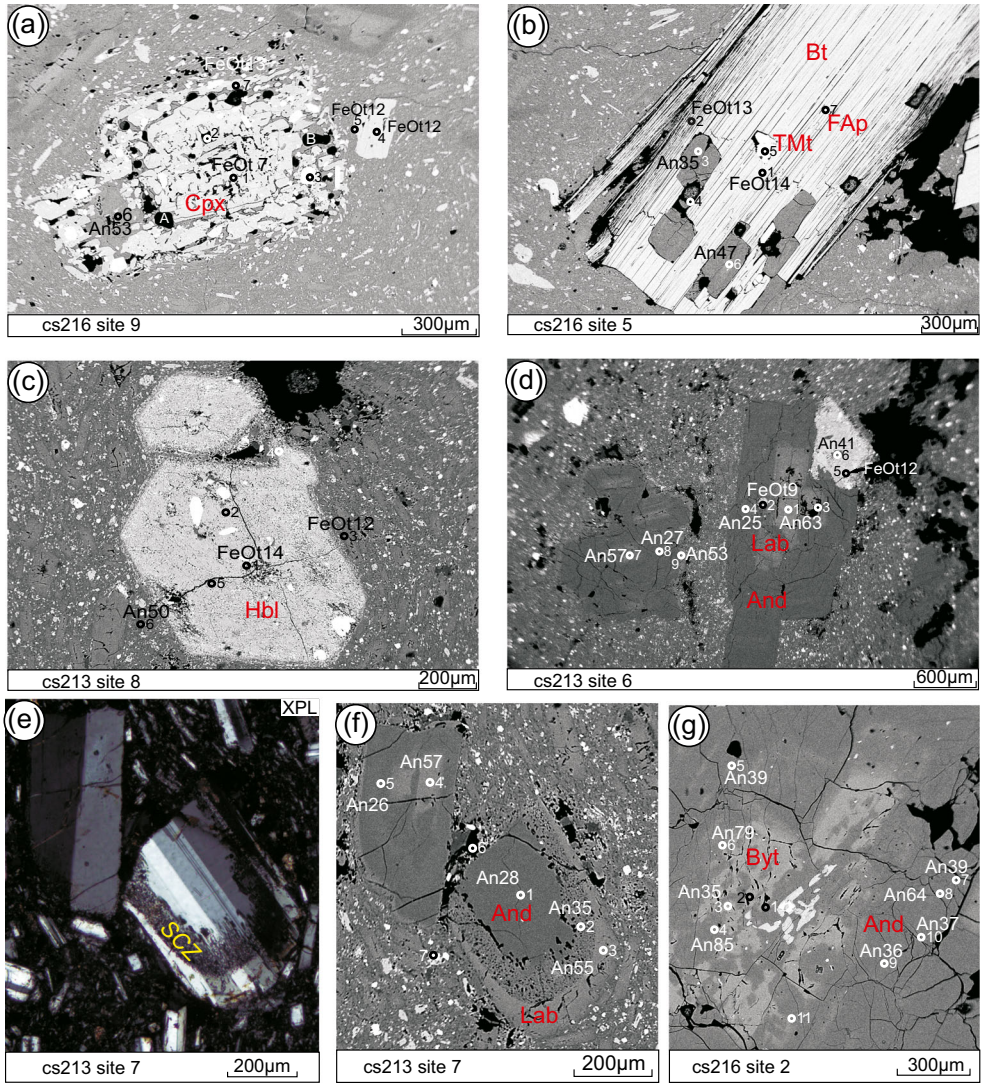

Fig. 11 Andesite mineral textures. Abbreviations as in Fig. 10. **a** Clinopyroxene crystal with dissolution voids (2) and a line of bubbles around its margin (positions A, B). The crystal is surrounded by a rim made up of titanomagnetite (3), labradorite (6), and orthopyroxene (7). This texture suggests either magma mixing, or that the clinopyroxene is a xenocryst. **b** Sample CS216 site 5 (SEM). Biotite phenocryst (1, 2) with reverse zoning and titanomagnetite (5), F-apatite (7), and andesine (3, 6) inclusions with dissolution voids (4). **c** Normally zoned magnesiohornblende phenocryst (1) with dissolution voids and inclusions of F-apatite (2). **d** Zoned plagioclase phenocryst with a labradorite core (1) with voids (3) to oligoclase (4) with magnesiohornblende inclusions (2). Phenocryst of oligoclase (8) with calcic spikes and patches of labradorite (7). Magnesiohornblende phenocryst (5) with andesine (6) inclusions. **e** Microphotograph under XPL. Two plagioclase phenocrysts. One with a spongy cellular zone close to the rim. Both show twinning and are zoned. **f** Plagioclase phenocryst with a spongy cellular zone close to the rim. The core is oligoclase (1), the spongy zone (2) consists of voids, andesine, and likely glass, and the clear rim is labradorite (3). A second phenocryst consists of a labradorite core (4) surrounded by oligoclase (5) and likely a calcic rim (bright). **g** Andesine phenocryst with patchy inclusions of bytownite (4, 6), magnesiohornblende (1), and titanomagnetite (2)

of Allen 1998 in Pachia and Kos). The only highstand comparable with the late Holocene was the MIS 5e or Tyrrhenian highstand. Molluscs from a terrace in northern Pyrgousa gave ages ranging from 114 ± 53 to 31 ± 11 ka by electron spin resonance dating (Blackwell et al. 2016). The older ages are consistent within error with the maximum highstand in MIS 5e, the youngest ages correspond to MIS 3. In the southern part of the islet, there has been only minor post-Tyrrhenian tilting, with subsidence in the west and minor uplift in east. This suggests that the younger ages found by Blackwell et al. (2016) are perhaps questionable, as eustatic sea level fluctuated around − 50 m during most of MIS 3. The terrace limestone has played an important role in protecting the KPT deposits from erosion during the 100-ka-long, last-glacial lowstand. The KPT has been eroded away from the higher elevations of the islet above the limit of the limestone.

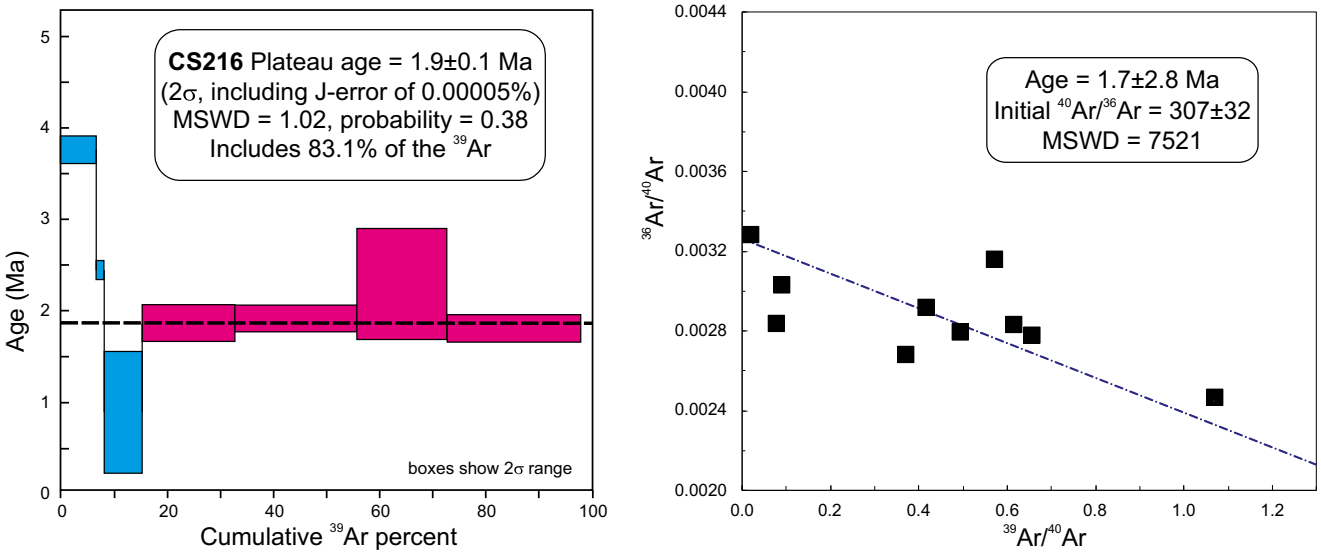

Fig. 12 Ar release spectra and isochron plot for andesite sample 216. Blue boxes indicate rejected data

Conclusions

Pyrgousa is underlain by complex domes, associated breccias, minor dykes, and probable flows of andesite that predate the Kos Plateau Tuff. Proximal facies of the KPT eruption on Pyrgousa (unit Dm of Allen et al. 1999) and the Tyrrhenian limestone terrace in the west of the islet are documented for the first time. Biotite from one sample of andesite gave a $^{40}Ar/^{39}Ar$ date of 1.9 ± 0.1 Ma, probably a maximum age because of excess ^{40}Ar. The andesites, and minor basaltic andesites, are enriched in Ba and Sr and resemble potassic rocks found elsewhere in the SE Aegean. They are interpreted to have formed by 5–10% partial melting of enriched SCLM in the stability field of phlogopite, amphibole, and garnet. They contrast with literature reports of magmas produced at the time of the KPT eruption at 0.16 Ma, and subsequently in the late Quaternary stratovolcano of Nisyros, derived principally from depleted asthenospheric mantle with trace elements derived from subducted Nile sediment.

An analogous transition from small magma volumes from SCLM forming andesite-dacite domes, followed by a voluminous explosive eruption and growth of small stratovolcanoes from magma derived from asthenospheric mantle, is seen on Methana in the northwestern South Aegean Arc. Such early andesite magmas play an important role in heating the upper crust, allowing growth and filling of upper crustal magma chambers as the supply of asthenospheric magma increased.

Acknowledgments Reviews by Olivier Bachmann, an anonymous reviewer, and Editor Katharine Cashman were extremely helpful and much appreciated.

Funding information Access to the islet was supported by University of Athens funding to GA. Petrological and geochemical analyses at Saint Mary's University were funded by a Discovery Grant to GPP from the Natural Sciences and Engineering Research Council of Canada.

References

Allen SR (1998) Volcanology of the Kos Plateau Tuff, Greece: the product of an explosive eruption in an archipelago. Ph.D. thesis, Monash University, Australia

Allen SR (2001) Reconstruction of a major caldera-forming eruption from pyroclastic deposit characteristics: Kos Plateau Tuff, eastern Aegean Sea. J Volcanol Geoth Res 105:141–162

Allen SR, Stadlbauer E, Keller J (1999) Stratigraphy of the Kos Plateau Tuff: product of a major Quaternary rhyolitic eruption in the eastern Aegean, Greece. Int J Earth Sci 88:132–156

Bachmann O, Huber C (2016) Silicic magma reservoirs in the Earth's crust. Am Min 101(11):2377–2404

Bachmann O, Charlier BLA, Lowenstern JB (2007) Zircon crystallization and recycling in the magma chamber of the rhyolitic Kos Plateau Tuff (Aegean arc). Geology 35:73–76

Bachmann O, Schoene B, Schnyder C, Spikings R (2010a) $^{40}Ar/^{39}Ar$ and U/Pb dating of young rhyolites in the Kos-Nisyros volcanic complex, Eastern Aegean Arc (Greece): age discordance due to excess ^{40}Ar in biotite. Geochem Geophys Geosyst 11:Q0AA08

Bachmann O, Wallace PJ, Bourquin J (2010b) The melt inclusion record from the rhyolitic Kos Plateau Tuff (Aegean arc). Contr Min Pet 159(2):187–202

Bachmann O, Deering CD, Ruprecht JS, Huber C, Skopelitis A, Schnyder C (2012) Evolution of silicic magmas in the Kos-Nisyros volcanic center, Greece: a petrological cycle associated with caldera collapse. Contr Min Pet 163:151–166

Barker SJ, Wilson CJ, Allan AS, Schipper CI (2015) Fine-scale temporal recovery, reconstruction and evolution of a post-supereruption magmatic system. Contr Min Pet 170(1):5 **(40 p)**

Bellon H, Jarrige J-J (1979) Le magmatisme néogène et quaternaire de l'île de Kos (Grèce): données géochronologiques. C R Acad Sci Paris D228:1359–1362

Blackwell BA, Skinner AR, Blickstein JI, Montoya AC, Florentin JA, Baboumian SM, Ahmed IJ, Deely AE (2016) ESR in the 21st

century: from buried valleys and deserts to the deep ocean and tectonic uplift. Earth Sci Rev 158:125–159

Buettner A, Kleinhanns IC, Rufer D, Hunziker JC, Villa IM (2005) Magma generation at the easternmost section of the Hellenic Arc: Hf, Nd, Pb and Sr isotope geochemistry of Nisyros and Yali volcanoes (Greece). Lithos 83:29–46

Di Paola GM (1974) Volcanology and petrology of Nisyros Island (Dodecanese, Greece). Bull Volc 38:944–987

Elburg MA, Smet I, De Pelsmaeker E (2014) Influence of source materials and fractionating assemblage on magmatism along the Aegean arc, and implications for crustal growth. Geol Soc London Spec Publ 385:137–160

Francalanci L, Varekamp JC, Vougioukalakis G, Defant MJ, Innocenti F, Manetti P (1995) Crystal retention, fractionation and crustal assimilation in a convecting magma chamber, Nisyros Volcano, Greece. Bull Volc 56:601–620

Hunzicker JC, Marini L (2005) The geology, geochemistry and evolution of Nisyros Volcano (Greece). In: Implications for the volcanic hazards. Mém Géol (Lausanne) 44, pp 1–192

IGME (2003) Geological map of Nisyros, scale 1:25 000

Klaver M, Djuly T, de Graaf S, Sakes A, Wijbrans J, Davies G, Vroon P (2015) Temporal and spatial variations in provenance of eastern Mediterranean Sea sediments: implications for Aegean and Aeolian arc volcanism. Geochim Cosmochim Acta 153:149–168

Klaver M, Matveev S, Berndt J, Lissenberg CJ, Vroon PZ (2017) A mineral and cumulate perspective to magma differentiation at Nisyros Volcano, Aegean arc. Contr Min Pet 172(11–12):95 **(23 p)**

Lange RA, Frey HM, Hector J (2009) A thermodynamic model for the plagioclase-liquid hygrometer/thermometer. Am Min 94(4):494–506

Lipman PW (2007) Incremental assembly and prolonged consolidation of Cordilleran magma chambers: evidence from the Southern Rocky Mountain volcanic field. Geosphere 3(1):42–70

Lowe DR (1975) Water escape structures in coarse-grained sediments. Sedimentology 22(2):157–204

Matsuda J, Senoh K, Maruoka T, Sato H, Mitropoulos P (1999) K-Ar ages of the Aegean volcanic rocks and their implication for the arc-trench system. Geochem J 33:369–377

Nomikou P, Papanikolaou D, Dietrich VJ (2018) Geodynamics and volcanism in the Kos-Yali-Nisyros volcanic field. In: Dietrich VJ, Lagios E (eds) Nisyros Volcano, active volcanoes of the world. Springer, Berlin, pp 13–55. https://doi.org/10.1007/978-3-319-55460-0_2

Pasteels P, Kolios N, Boven A, Saliba E (1986) Applicability of the K-Ar method to whole rock samples of acid lava and pumice: case of the upper Pleistocene domes and pyroclastics of Kos Island, Aegean Sea, Greece. Chem Geol 57:145–154

Pe-Piper G, Moulton B (2008) Magma evolution in the Pliocene Pleistocene succession of Kos, South Aegean arc (Greece). Lithos 106:110–124

Pe-Piper G, Piper DJW (2002) The igneous rocks of Greece. Gebrüder Borntraeger, Berlin

Pe-Piper G, Piper DJW (2007) Upper-Miocene igneous rocks of Samos: the role of tectonism in petrogenesis in the southeastern Aegean. Geol Soc London Spec Publ 291:75–97

Pe-Piper G, Piper DJW (2013) The effect of changing regional tectonics on an arc volcano: Methana, Greece. J Volc Geotherm Res 260:146–163

Pe-Piper G, Piper DJW, Wang Y, Zhang Y, Trottier C, Ge C, Yin Y (2016) Quaternary evolution of the rivers of northeast Hainan Island, China: tracking the history of avulsion from mineralogy and geochemistry of river and delta sands. Sed Geol 333:84–99

Piper DJW, Pe-Piper G, Lefort D (2010) Precursory activity of the 161 ka Kos Plateau Tuff eruption, Aegean Sea (Greece). Bull Volc 72(6):657–669

Ridolfi F, Renzulli A, Puerini M (2010) Stability and chemical equilibrium of amphibole in calc-alkaline magmas: an overview, new thermobarometric formulations and application to subduction-related volcanoes. Contr Min Pet 160(1):45–66

Smet I (2014) Spatial and temporal petrological-geochemical variations in the volcanic rocks of the Saronic Gulf (West Aegean arc, Greece): influence of local geodynamic parameters on magma genesis. PhD thesis, Ghent University, Belgium, 349 p

Vanderkluysen L, Volentik A, Hernandez J, Hunzicker JC, Bussy F, Principe C (2005) The petrology and geochemistry of lavas and tephras of Nisyros Volcano (Greece). Mem Géol (Lausanne) 44:79–99

Whitney DL, Evans BW (2010) Abbreviations for names of rock-forming minerals. Amer Min 95:185–187

Wyers GP, Barton M (1989) Polybaric evolution of calc-alkaline magmas from Nisyros, southeastern Hellenic Arc, Greece. J Petrol 30:1–37